Pflugers Arch - Eur J Physiol (2017) 469:1163–1176
DOI 10.1007/s00424-017-1970-6

SIGNALING AND CELL PHYSIOLOGY

Interleukin-13 increases pendrin abundance to the cell surface in bronchial NCI-H292 cells via Rho/actin signaling

Annamaria Russo[1] · Marianna Ranieri[1] · Annarita Di Mise[1] · Silvia Dossena[2] · Tommaso Pellegrino[1] · Emilia Furia[3] · Charity Nofziger[2] · Lucantonio Debellis[1] · Markus Paulmichl[2] · Giovanna Valenti[1,4,5] · Grazia Tamma[1,4]

Received: 4 January 2017 / Revised: 20 March 2017 / Accepted: 22 March 2017 / Published online: 4 April 2017

Abstract Interleukin-13 (IL13) is a major player in the development of airway hyperresponsiveness in several respiratory disorders. Emerging data suggest that an increased expression of pendrin in airway epithelia is associated with elevated airway hyperreactivity in asthma. Here, we investigate the effect of IL13 on pendrin localization and function using bronchiolar NCI-H292 cells. The data obtained revealed that IL13 increases the cell surface expression of pendrin. This effect was paralleled by a significant increase in the intracellular pH, possibly via indirect stimulation of NHE. IL13 effect on pendrin localization and intracellular pH was reversed by theophylline, a bronchodilator compound used to treat asthma. IL13 upregulated RhoA activity, a crucial protein controlling actin dynamics, via G-alpha-13. Specifically, IL13 stabilized actin cytoskeleton and promoted co-localization and a direct molecular interaction between pendrin and F-actin in the plasma membrane region. These effects were reversed following exposure of cells to theophylline. Selective inhibition of Rho kinase, a downstream effector of Rho, reduced the IL13-dependent cell surface expression of pendrin. Together, these data indicate that IL13 increases pendrin abundance to the cell surface via Rho/actin signaling, an effect reversed by theophylline.

Keywords Pendrin · IL13 · Actin · Rho signaling · Asthma · COPD

Annamaria Russo and Marianna Ranieri contributed equally to this work.

✉ Marianna Ranieri
marianna.ranieri@uniba.it

✉ Grazia Tamma
grazia.tamma@uniba.it

[1] Department of Biosciences Biotechnologies and Biopharmaceutics, University of Bari, Via Orabona 4, 70125 Bari, Italy

[2] Institute of Pharmacology and Toxicology, Paracelsus Medical University, Salzburg, Austria

[3] Department of Chemistry and Chemical Technologies, University of Calabria, Rende, Italy

[4] Istituto Nazionsale di Biostrutture e Biosistemi (I.N.B.B.), Rome, Italy

[5] Centre of Excellence Genomic and Proteomics GEBCA, University of Bari, Bari, Italy

Introduction

Pendrin (SLC26A4) is a member of the SLC26 (solute carrier 26) family and functions as an anion exchanger for monovalent anions including iodide, chloride, bicarbonate, hydroxide, and thiocyanate [41, 53]. This protein is mainly expressed in the inner ear, thyroid, and kidney [32, 43, 51]. A relatively lower expression of pendrin has been described in other organs such as the mammary gland, testis, endometrium, liver, and lung [15, 17, 53]. Lung expression of pendrin was first described in transgenic mouse models of asthma induced by the overexpression of the Th2 cytokine interleukin-13 (IL13) [31]. A correlation between pendrin expression and several respiratory disorders such as asthma, chronic obstructive pulmonary disease (COPD), rhinovirus, and *Bordetella pertussis* infection has been described [27, 39, 49]. In the respiratory system, pendrin reabsorbs Cl^- against HCO_3^- or thiocyanate (SCN^-), which is oxidized by H_2O_2 in hypothiocyanite, having an antimicrobial activity in airway surface liquid (ASL) [19, 41]. Balanced chloride and bicarbonate transport is important to modulate fluid secretion and to pH regulation. In fact, loss of activity of cystic fibrosis transmembrane conductance regulator (CFTR), an anion channel that facilitates HCO_3^- transport, decreases airway surface pH, thus preventing bacterial killing [42]. Within the

respiratory epithelium, airway surface hydration depends closely on the expression of selective water and ion channels [21, 30]. Deregulated expression and/or channel activity may contribute to the lung diseases [3]. COPD and asthma both damage lung functions. COPD is the third leading cause of death worldwide after ischaemic heart disease and stroke [35] and is associated with obstruction of the lung due to a chronic and irreversible inflammatory condition [52]. Asthma is a heterogeneous syndrome displaying different clinical phenotypes characterized by reversible lung obstruction, bronchial hyperresponsiveness, and airway inflammation [36].

Besides IL4 and IL5, IL13 plays a crucial role in determining airway inflammation and hyperresponsiveness [29], and increased airway narrowing is the main symptom characterizing these disorders. However, the molecular mechanisms promoting airway inflammation and hyperresponsiveness remain unclarified. Abnormal contractile properties of airway smooth muscle cells play a pivotal role in the development of these diseases. IL13 is a key mediator of Rho-dependent calcium sensitization in smooth muscle contraction [9]. Importantly, IL13 can act also on airway epithelial cells, where it stimulates the signal transducer and activator of transcription factor 6 (STAT6) [31]. STAT6 activation, via IL13 pathway, results in a significant increase of the expression level of pendrin [39, 40].

Management of the abovementioned respiratory diseases is very complex due to the heterogeneity of responses to treatment. Antibodies targeting the IL13 receptor have been tested in patients with severe asthma, though clinical follow-up demonstrated their inefficacy [5]. On the other hand, lebrikizumab, a monoclonal antibody to IL13, ameliorated lung functions within 12 weeks [11]. Alternatively, a selective inhibitor of Rho signals have been also preliminary tested because Rho kinase inhibition decreases inflammation and mucus hypersecretion [50, 63], even though the molecular signals controlled by the Rho-dependent pathway are not clarified yet. In this scenario, an improved understanding of the downstream effectors in the IL13 pathway is an unmet need, and is essential to the identification of novel therapeutic targets. Here, we found that IL13 treatment increases the abundance of pendrin at the plasma membrane via Rho/actin signaling, an effect counteracted by theophylline, a known bronchodilator compound used to treat asthma. These observations may contribute to elucidate the pathogenesis of lung diseases in which pendrin may represent a novel therapeutic target.

Methods

Chemicals and reagents

All chemicals were purchased from Sigma (Sigma-Aldrich, Milan, Italy). 2′,7′-bis(carboxyethyl)-5(6)-carboxyfluorescein acetoxymethyl ester (BCECF-AM), media, sera for cell culture, Alexa 555 and Alexa 488-conjugated antibodies, were purchased from Life Technologies (Life Technologies, Monza, Italy). Mirus TransIT®-2020 transfection reagent was purchased from Tema Ricerca (Tema Ricerca s.r.l. Bologna, Italy). Biocytin hydrazide and streptavidin beads were purchased from EZ-Link® Pierce. Anti-Pendrin (H-195), anti-G-alpha-13, and HRP-linked goat anti-rabbit antibodies were from Santa Cruz (D.B.A. Italia s.r.l. Milano).

Plasmids

Plasmids were already described [59]. Briefly, the open reading frame (ORF) of human pendrin (PDS) isolated from the thyroid was subcloned into the XhoI and BamHI restriction sites of the pECFPN1 (Clontech) vector. When transfected into mammalian cells, this construct leads to the production of pendrin with a C-terminal ECFP tag (PDS-ECFP). Alternatively, pECFPC1-pendrin, coding for pendrin with an N-terminal ECFP tag (ECFP-PDS), was used. The pEYFP-Mem construct was from Clontech. Transfection of cells with this construct results in a strong labeling of the plasma membrane. The construct pEYFPN1-Actin was kindly gifted by Dr. Bazzini (University of Milan, Italy). Rho activity was evaluated using the probe Raichiu-RBD (RhoA-binding domain with ECFP and EYFP fused to the N and C terminus, respectively) [65].

Cell culture and transfection

NCI-H292 cells (from ATCC) were grown in Advanced RPMI 1640 Media supplemented with 10% (*v*/*v*) fetal bovine serum, 100 i.u./ml penicillin and 100 μg/ml streptomycin at 37 °C with 5% CO2. Cells were seeded and grown on filters for cell surface biotinylation and for spectrophotometric measurements of bicarbonate. Otherwise, cells were seeded on plastic dishes or coverslips. After seeding for 24 h (~80% confluence), cells were transiently transfected with plasmids (0.4 μg of DNA/cm^2) using TransIT®-2020 transfection reagent (0.75 μl/cm^2) according to the protocol provided by the manufacturer (Mirus, Mirus Bio LLC, USA). Experiments were performed 48 h post-transfection.

Treatments

NCI-H292 cells were incubated with IL13 (50 ng/ml) for 24 h, theophylline (10 μg/ml) for 8 h, or the vehicle (control). Further, cells were treated with IL13 (50 ng/ml) for 24 h in the presence of theophylline (10 μg/ml) for the last 8 h.

Video imaging measurements

For intracellular pH measurements, the coverslips with cells were mounted in a perfusion chamber (FCS2 Closed Chamber System, BIOPTECHS, Butler, U.S.A.) and measurements

were performed using an inverted microscope (Nikon Eclipse TE2000-S), equipped for single-cell fluorescence measurements and imaging analysis. The sample was illuminated through a ×40 oil immersion objective (NA = 1.30).

FRET measurements

NCI-H292 cells were co-transfected (transiently) with PDS-ECFP and EYFP-Mem or with ECFP-PDS and Actin-EYFP. Alternatively, cells were transfected with ECFP-Raichu-RBD-EYFP. Forty-eight hours after transfection and treatments, cells were fixed with 4% paraformaldehyde (PFA) in PBS (pH 7.4) for 20 min at room temperature and washed three times in PBS. Afterwards, coverslips with cells were mounted in Mowiol (polyvinyl alcohol 4-88; Sigma-Aldrich, Milan, Italy). Visualization of ECFP- and/or EYFP-expressing cells and detection of FRET were performed on an inverted microscope (Nikon Eclipse TE2000-S), equipped with a monochromator controlled by MetaMorph/MetaFluor software. ECFP was excited at 433 nm and EYFP at 512 nm. All images were aligned and corrected for background in the emission windows for FRET (535/30 nm), ECFP (475/30 nm), and EYFP (535/26 nm). Each image was further corrected for ECFP crosstalk and EYFP cross-excitation as shown by Rodighiero et al. [47]. Thus, netFRET = [IFRETbg − ICFPbg × k1 − IYFPbg (K2 − αK1)]/(1 − K1δ), where IFRETbg, ICFPbg, and IYFPbg are the background-corrected pixel gray values measured in the FRET, ECFP, and EYFP windows, respectively; K1, K2, α, and δ are calculated to evaluate the crosstalk between donor and acceptor. The obtained netFRET values were normalized for the expression levels of ECFP and EYFP (NFRET = netFRET × 100/(ICFPbg × IYFPbg)$^{1/2}$). The integrated fluorescence density values of the images from ten regions of interest in each cell [46], close to the cells' outer margins, were analyzed using MetaMorph and Microsoft Excel softwares.

Cell surface biotinylation

Biotinylation was carried out as already described [57]. Shortly, NCI-H292 cells were cultured on six-well filters in complete growing medium and transfected with PDS-ECFP. After treatments, cells were washed thoroughly with an ice-cold coupling buffer (0.1 M $NaPO_3$, 0.15 M NaCl, pH 7.2) before being subjected to oxidation with 20 mM Na-meta-periodate in an oxidation buffer for 30 min on ice in the dark. Following three rounds of washing with the coupling buffer, cell surface glycoproteins were labeled with 5 mM Biocytin hydrazide (EZ-Link® Pierce) for 30 min. The biotinylation buffer was removed and cells were incubated with a quenching solution (50 mM NH_4Cl in PBS, pH 7.2) for 5 min and washed three times with the coupling buffer. Cells were solubilized with lysis buffer (1% Triton X-100, 0.01% SDS in PBS supplemented with 2 μg/ml pepstatin, 2 μg/ml leupeptin, and 2 mM PMSF) for 30 min. The lysates were homogenized using an ultrasonic homogenizer at 40 Hz for 20 s and centrifuged at 12,000×*g* for 20 min. An aliquot of the supernatants (30 μl) was diluted in Laemmli buffer containing 8 M Urea. The remaining biotinylated proteins were pulled down with immobilized streptavidin beads. The complexes were washed 3 times with wash buffer (0.5% Triton X-100, 0.01% SDS in PBS), denatured in a Laemmli buffer containing 8 M Urea for 5 min at 90 °C, separated by SDS-PAGE and immunoblotted with anti-pendrin antibodies (1:500 dilution).

Intracellular pH measurements

NCI-H292 cells were loaded with 2 μM BCECF-AM for 30 min at 37 °C in Dulbecco's modified Eagle's medium and then washed in Ringer's solution containing (in mmol/L) 130 NaCl, 3 KCl, 0.5 $MgCl_2$, 1.2 $NaHCO_3$, 10 glucose, 1.2 $CaCl_2$, 10 HEPES, and pH 7.4. BCECF was excited at 490 and 440 nm. Emitted fluorescence was passed through a single-band dichroic mirror and filtered at 535 nm (Omega Optical, Brattleboro, VT, USA). The BCECF fluorescence intensity ratio was calibrated with solutions containing 10 μM nigericin and high potassium (in mmol/L 5 NaCl, 130 KCl, 0.1 $MgCl_2$, 10 glucose, 1.2 $CaCl_2$, 10 HEPES, and pH 5.30, 6.2, 7.4, and 8.45 adjusted with KOH or HCl).

Immunofluorescence and F-actin visualization

Immunocytochemistry was performed as previously described [58]. Briefly, NCI-H292 cells were grown, transfected with PDS-ECFP, treated as described, and fixed for 30 min with 4% paraformaldehyde in PBS. Cells were permeabilized with 0.1% Triton X-100 in PBS for 5 min, blocked with 1% BSA in PBS for 30 min, and incubated for 2 h with anti-pendrin antibodies (raised in rabbit, 1:500 dilution). After washing, cells were incubated with goat anti-rabbit antibodies coupled to Alexa-555 (1:3000 dilution).

To detect pendrin in co-localization experiments, the secondary antibody was coupled to Alexa-488 (1:3000 dilution). To detect F-actin, specimens were further incubated with TRITC-conjugated phalloidin (400 μg/ml) for 45 min and subsequently washed.

The coverslips were mounted on glass slides with Mowiol mounting medium. The fluorescence signals were detected by a confocal microscope (Leica TCS SP2, Leica Microsystems, Heerbrugg, Switzerland).

F-actin co-sedimentation assay

F-actin co-sedimentation was performed as described previously [60]. Briefly, total membrane and cytosol fractions were prepared from NCI-H292 cells. Cells were scraped and resuspended in homogenization buffer that contained 20 mM Tris-

HCl (pH 8.0), 1 mM EDTA, 1 mM dithiothreitol, and protease inhibitors. Cells were homogenized using a 27-gauge needle, and nuclei were removed by centrifugation at 800×*g* for 10 min. Membrane and cytosol fractions were obtained by centrifugation for 1 h at 4 °C at 150,000×*g*. Cytosolic proteins (800 μg each conditions) were used for F-actin polymerization. Specifically, formation of F-actin was initiated using a 50-fold polymerization buffer that contained 200 mM $MgCl_2$, 4 M KCl, and 100 mM ATP. The samples were incubated for 1 h at 37 °C, and F-actin was pelleted by ultracentrifugation for 1 h at 4 °C at 150,000×*g*. The F-actin-containing pellets were rinsed with homogenization buffer.

Cytosol and F-actin fractions were separated by 13% SDS-PAGE and immunoblotted with G-alpha 13-specific antibodies.

Statistical analysis

One-way ANOVA followed by multiple comparison tests was used for the statistical analysis. When applicable, *t* test was also used. All values are expressed as means ± SEM. A value of $P < 0.05$ was considered as statistically significant.

Results

IL13 stimulates pendrin trafficking to the plasma membrane in bronchiolar NCI-H292 cells

The effect of IL13 exposure on pendrin localization was evaluated in epithelial NCI-H292 cells by confocal microscopy (Fig. 1). Treatment with IL13 (50 ng/ml) increased the cell surface abundance of pendrin (white arrows indicate the plasma membrane in IL13-treated cells) compared with untreated cells (control). Co-treatment with theophylline (10 μg/ml), a classical bronchodilator drug, abolished IL13 action, and pendrin staining appeared similar to that observed in control cells. Incubation with theophylline alone did not alter the cellular distribution of pendrin compared to control.

To quantify pendrin abundance at the plasma membrane, FRET studies were performed as previously described [59]. NCI-H292 cells were co-transfected with constructs leading to the expression of pendrin C-terminally tagged with ECFP (PDS-ECFP), and EYFP-Mem (a marker of the plasma membrane, see the "Methods" section) and treated with IL13 and/or theophylline. Experiments were executed 48 h post-transfection on specimens showing a transfection efficacy of 40–45%. NFRET was calculated in fixed cells in ten regions near the outer perimeter of each cell; the values were corrected as described by Rodighiero [47]. When the two fusion proteins PDS-ECFP and EYFP-Mem are in close proximity to each another, FRET signal increases due to the transfer of resonance energy from the donor (PDS-ECFP) to the acceptor (EYFP-Mem). With the ECFP-EYFP FRET pair, statistically significant NFRET variations ranging from 10 to 20% are generally considered biologically relevant [7]. Compared to control, exposure of cells to IL13 significantly increased FRET signal, consistent with an augmented abundance of pendrin at the plasma membrane (IL13, 109.9 ± 2.319, $n = 211$ cells vs. CTR, 100 ± 1.347, $n = 250$ cells, $^*p < 0.001$ vs. CTR Fig. 2a). Theophylline reversed IL13-dependent accumulation of pendrin at the plasma membrane (IL13-Theo, 97.03 ± 3.480, $n = 67$ cells, Fig. 2a). Incubation with theophylline alone did not exert any relevant change on the cellular distribution of pendrin (Theo, 94.87 ± 3.480, $n = 84$ cells, Fig. 2a). Data are also shown as frequency distribution histogram of the relative changes of NFRET under the described conditions (Fig. 2b).

To verify whether the IL13-dependent increase in the localization of pendrin at the cell surface observed by confocal imaging and FRET analysis involved the insertion into

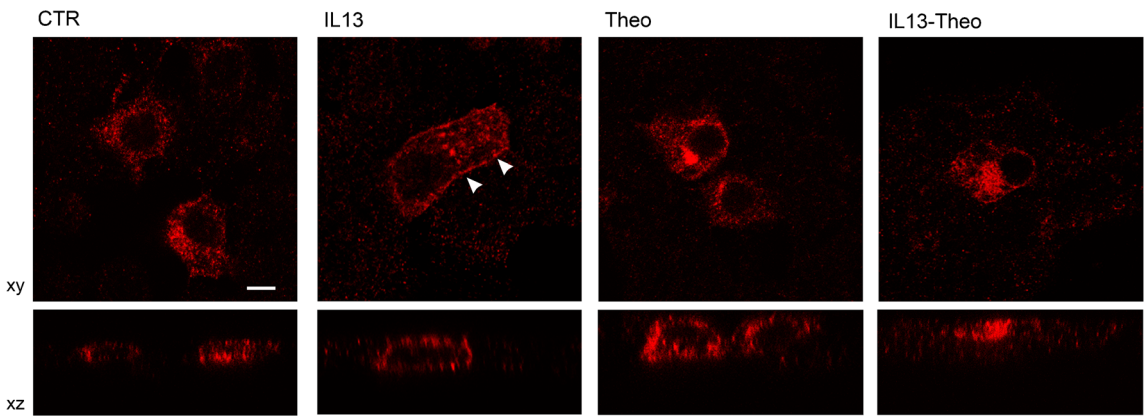

Fig. 1 Confocal analysis of pendrin localization in NCI-H292 cells. Cells were transfected with pendrin, treated with the vehicle (CTR), IL13 (50 ng/ml for 24 h), theophylline (Theo, 10 μg/ml for 8 h), or IL13 in the presence of theophylline (IL13-Theo; 50 ng/ml IL13 for 24 h in the presence of 10 μg/ml theophylline for the last 8 h) and processed for immunocytochemistry. *Scale bar* 5 μM

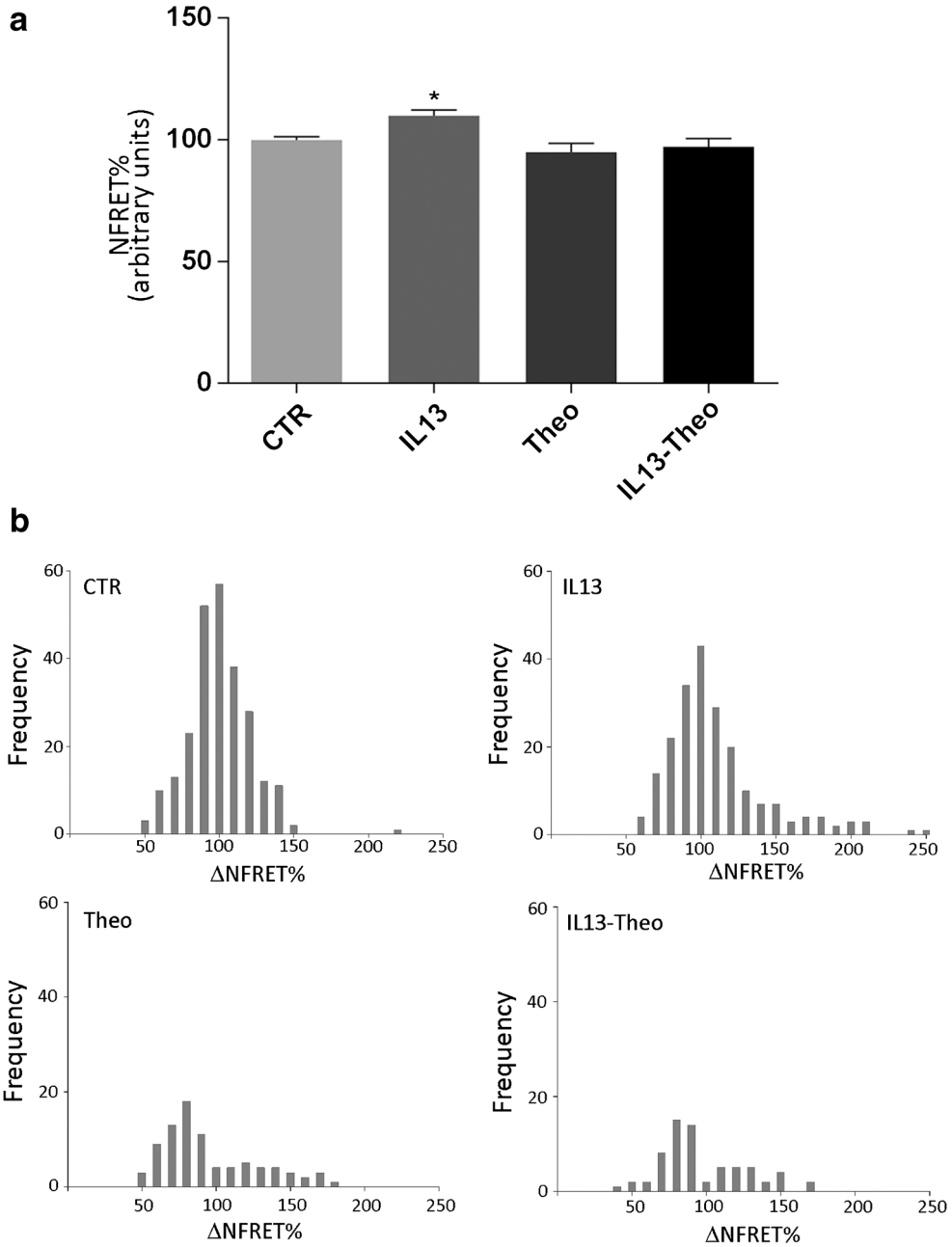

Fig. 2 Evaluation of pendrin expression at the plasma membrane by FRET studies. **a** NCI-H292 cells were transiently transfected with PDS-ECFP and EYFP-Mem. FRET experiments were performed 48 h after transfection. Histograms show NFRET measured in cells treated with the vehicle (CTR) or stimulated with IL13 (50 ng/ml for 24 h), theophylline (Theo, 10 μg/ml for 8 h), or IL13 and theophylline (IL13-Theo; 50 ng/ml IL13 for 24 h in the presence of 10 μg/ml theophylline for the last 8 h). (*$p < 0.001$ vs. CTR). **b** Frequency distribution histograms of the relative changes of NFRET in percent, under basal condition (CTR), IL13 stimulation, theophylline (Theo), and co-treatment with IL13 and theophylline (IL13-Theo). The obtained data were collected from ten regions of interest (ROI) located near the plasma membrane

the plasma membrane, cell surface biotinylation experiments were performed in cells transiently expressing pendrin (Fig. 3a). To increase the yield of the detectable membrane-inserted pendrin [4], the cell surface was labeled with biocytin hydrazide which binds glycoproteins specifically. In contrast, conventional biotinylation reagents bind lysine residues, which may be poorly accessible from the extracellular side [57–59, 62]. The amount of membrane-inserted pendrin, labeled with biocytin hydrazide, was normalized to the total cellular amount of pendrin. In line with immunofluorescence and FRET data, IL13 significantly increased the cell surface expression of pendrin (IL13, 1.879 ± 0.2550, $p < 0.05$ vs. CTR, $n = 5$ *$p = 0.0045$). Importantly, the IL13-dependent increase of pendrin abundance at the plasma membrane was abolished when cells were co-treated with theophylline (IL13-Theo, 0.9079 ± 0.1226, $n = 5$). Compared to untreated cells, incubation with theophylline alone (Theo, 1.083 ± 0.2084, $n = 5$) did not affect the membrane insertion of pendrin (Fig. 3a–b). The specificity of anti-pendrin antibodies was evaluated by Western blotting on protein extracts from untransfected (mock) and pendrin expressing cells (Fig. 3c).

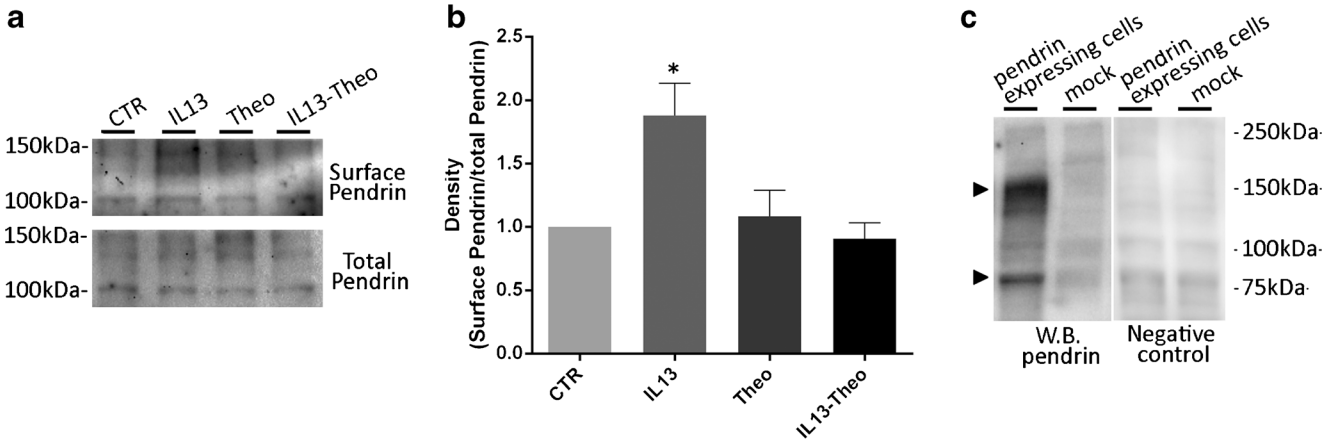

Fig. 3 **a** *Left*, representative pendrin immunoblot on biotinylated (*top panel*) and whole cell (*bottom panel*) proteins in NCI-H292 cells transiently transfected with PDS-ECFP. Cells were treated with the vehicle (CTR), IL13 (50 ng/ml for 24 h), theophylline (Theo, 10 μg/ml for 8 h), or IL13 and theophylline (IL13-Theo; 50 ng/ml IL13 for 24 h in the presence of 10 μg/ml theophylline for the last 8 h). **b** The histogram on the right shows the densitometry of specific bands in each lane (*p = 0.0045 vs. CTR). The relative amounts of pendrin upon each treatment were quantified from five independent experiments. **c** Western blotting to assess the specificity of the anti-pendrin antibody. Untransfected (mock) and pendrin expressing cells were assayed with or without (negative control) the anti-pendrin antibody. The *black arrows* indicate the specific bands used to semi-quantify the abundance of pendrin in the plasma membrane

IL13 stimulates pendrin activity in bronchiolar NCI-H292 cells

Previous studies documented a functional involvement of pendrin in controlling intracellular pH, owing on its activity as a Cl^-/HCO_3^- exchanger [21, 48, 59]. To evaluate whether the increased abundance of pendrin at the plasma membrane coincides with an increase in its activity, intracellular pH was measured (Fig. 4). To this end, NCI-H292 cells were transiently transfected with PDS-ECFP and loaded with the pH-sensitive dye BCECF-AM (2 μM for 30 min). Surprisingly, treatment with IL13 resulted in a significant intracellular alkalinization (IL13, 7.97 ± 0.0822, n = 56, vs. CTR, 7.37 ± 0.053, n = 33 *p < 0.0001) in pendrin-expressing cells. Co-treatment with theophylline counteracted IL13 by decreasing intracellular pH to a mean value not significantly different from that observed in control cells (IL13-Theo, 7.66 ± 0.073, n = 28). Theophylline alone did not alter intracellular pH. Moreover, mentioned treatments did not alter the intracellular pH in cells expressing the transfection marker ECFP (data not shown).

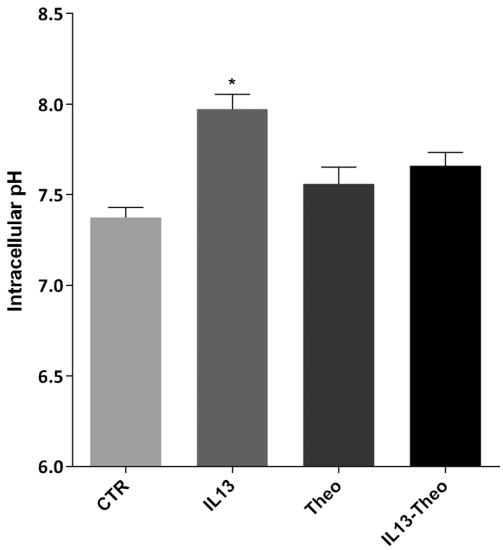

Fig. 4 Intracellular pH measured in NCI-H292 cells transiently transfected with PDS-ECFP. Cells were loaded with BCECF-AM (2 μM for 30 min). Histograms represent the intracellular pH after exposure of cells to the vehicle (CTR), IL13 (50 ng/ml for 24 h), theophylline (Theo, 10 μg/ml for 8 h), or IL13 and theophylline (IL13-Theo; (50 ng/ml IL13 for 24 h in the presence of 10 μg/ml theophylline for the last 8 h) (*p < 0.0001 vs. CTR)

In bronchial epithelial cells, IL13 promotes a secretory phenotype by reducing Na^+ reabsorption via ENaC and stimulating Cl^- secretion via CFTR [2], but the molecular mechanism modulating intracellular pH is not clarified yet. In hematopoietic FL5.12 and COS cells, IL7 and IL3 caused a significant cellular alkalinization by stimulating the activity of Na^+/H^+ exchanger NHE1 via p38 MAPK [28]. To evaluate the possible involvement of Na^+/H^+ exchange (NHE) on intracellular alkalinization following exposure to IL13, we measured changes of intracellular pH in the presence of 5-(N,N-dimethyl)-amiloride (DMA), a selective NHE inhibitor. NCI-H292 cells were treated as described above in the presence of DMA for 30 min and assayed for intracellular pH (Fig. 5). The difference between the intracellular pH measured in cells treated with DMA and IL13-DMA was significantly higher in PDS-expressing cells compared to untransfected cells (ΔpH = 0.442 ± 0.0473, n = 29 vs. untransfected cells ΔupH = 0.22 ± 0.007, n = 19 *p = 0.0001), therefore indicating that, following IL13 exposure, a greater intracellular acidification occurs in PDS-transfected cells. These findings led us to hypothesize that cells expressing pendrin display a higher

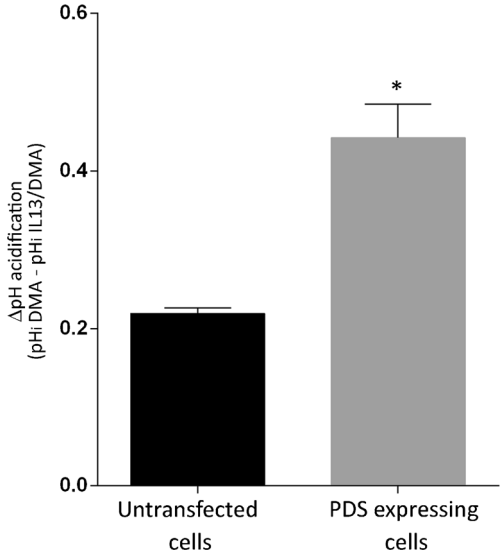

Fig. 5 Effect of IL13 (50 ng/ml for 24 h) on intracellular pH (pHi) under exposure to 5-(N,N-dimethyl)-amiloride (DMA). The pHi was measured in NCI-H292 cells untransfected or transiently transfected with PDS-ECFP loaded with BCECF (2 μM for 30 min). DMA (20 μM) was added 30 min before the experiment. Histograms represent the differences of intracellular pH variation calculated from cells treated with DMA alone and DMA in the presence of IL13 (ΔupH) (*p = 0.0001)

IL13-stimulated Cl^-/HCO_3^- exchange activity that only becomes apparent following inhibition of a compensatory Na^+/H^+ exchange activity.

IL13 stimulates Rho/actin signaling in bronchiolar NCI-H292 cells

The heterotrimeric G 13 proteins (G-alpha-13) stimulate NHE activity in several cell types [26, 61]. Therefore, to investigate the possible pathway by which IL13 causes intracellular alkalinization via NHE stimulation, G-alpha-13 involvement was evaluated by analyzing its affinity with F-actin, an index of G-alpha-13 activity [55, 60]. Cytosolic fractions of NCI-H292 cells were prepared, F-actin polymerization was induced, and F-actin-interacting proteins were analyzed by Western blotting (Fig. 6). The amount of G-alpha-13 in the F-actin-enriched fraction (active G-alpha-13) was normalized to the total amount of G-alpha-13 in the soluble fraction from which the F-actin-enriched fraction was obtained (see the "Methods" section). Relative to the control (Fig. 6), IL13 caused a significant increase in immune-detectable G-alpha-13 in the F-actin-enriched fraction (IL13, 1.617 ± 0.1930, *p = 0.027 vs. CTR, n = 3). Theophylline abolished IL13 action on G-alpha-13 affinity to F-actin (IL13, 1.617 ± 0.1930 vs. IL13-Theo, 0.7823 ± 0.1987, n = 3 #p = 0.0027).

It is known that G-alpha 12/13 activates RhoA, a small GTPase of the Rho family, which plays a role in controlling actin dynamics [54–56]. Rho activity was evaluated with FRET studies using a fluorescent probe (Raichu-RBD, see the "Methods" section) consisting of the Rho-binding domain (RBD) of Rhotekin sandwiched between EYFP and ECFP [65]. Binding of endogenous GTP-RhoA to RBD distances the FRET donor ECFP from the FRET acceptor EYFP, thereby decreasing FRET efficiency. IL13 decreased FRET signal, consistent with a significant upregulation of Rho activity (Fig. 7a). Theophylline prevented IL13 response on Rho functionality, as revealed by FRET values which were comparable to those measured in untreated cells. Data are also represented as frequency distribution histogram of the relative changes of netFRET under the described conditions (Fig 7b).

Theophylline treatment alone resulted in a significant increase in FRET signal, indicating downregulation of Rho activity. These data suggest that Rho proteins are involved in the signal transduction cascade activated by IL13.

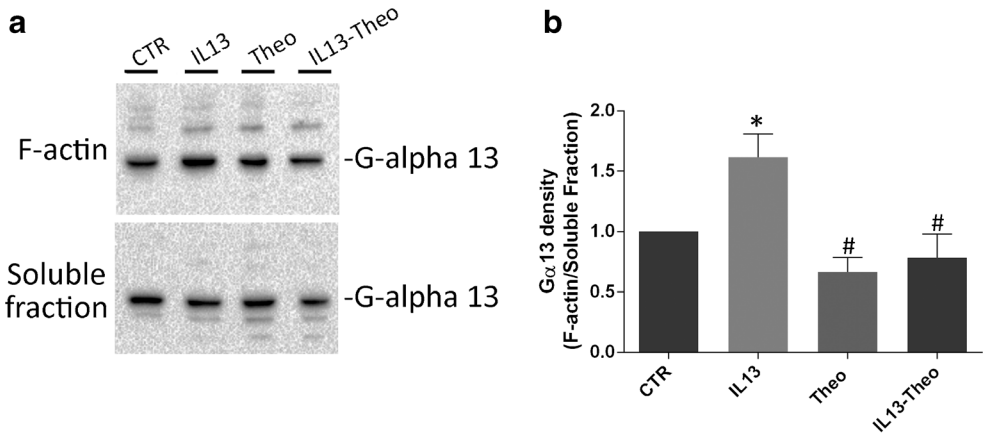

Fig. 6 G-alpha-13 and F-actin co-sedimentation. **a** Cytosolic fractions of NCI-H292 cells exposed to the vehicle (CTR), IL13 (50 ng/ml for 24 h), theophylline (Theo, 10 μg/ml for 8 h), or IL13 and theophylline (IL13-Theo; 50 ng/ml IL13 for 24 h in the presence of 10 μg/ml theophylline for the last 8 h) were prepared and F-actin polymerization was induced. F-actin-interacting proteins were analyzed by Western blotting. Equal amounts of F-actin fractions (30 μg/lane) were separated by SDS-PAGE and immunoblotted with an anti-G-alpha-13 antibody. **b** On the *right*, densitometric analysis of four independent experiments is shown (*p = 0.027 vs. CTR; #p = 0.0027 vs. IL13)

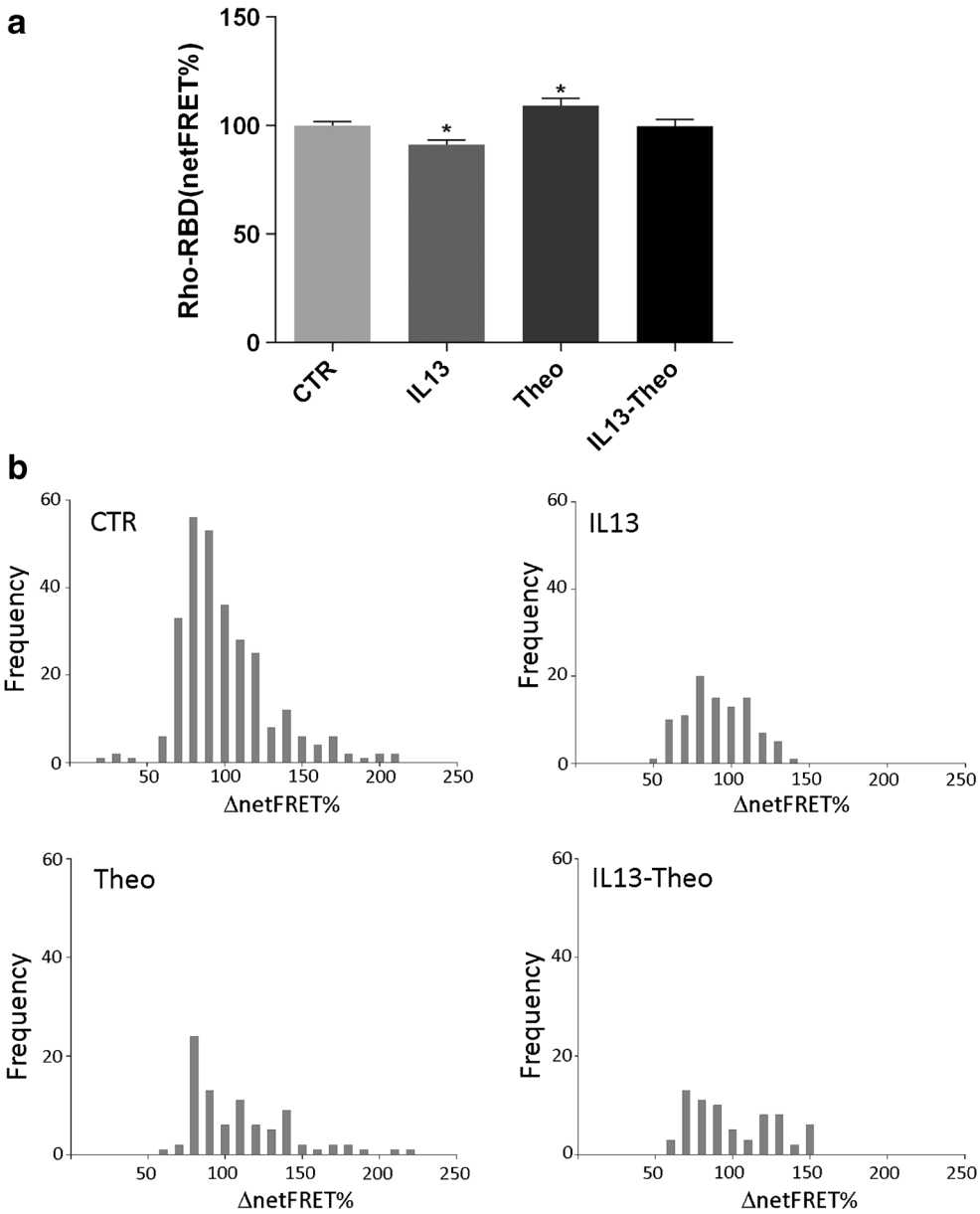

Fig. 7 Evaluation of Rho activity by FRET experiments. **a** NCI-H292 cells were transiently transfected with Raichiu-RBD as described in the "Methods" section. FRET experiments were performed 48 h after transfection. Histograms represent netFRET measured in cells treated with the vehicle (CTR) or stimulated with IL13 (50 ng/ml for 24 h), theophylline (Theo, 10 μg/ml for 8 h), or IL13 and theophylline (IL13-Theo; 50 ng/ml IL13 for 24 h in the presence of 10 μg/ml theophylline for the last 8 h). (*p = 0.008 vs. CTR). **b** Frequency distribution histograms of the relative changes of netFRET in percent, under basal condition (CTR), IL13 stimulation, theophylline (Theo), and co-treatment with IL13 and theophylline (IL13-Theo). The obtained data were collected from ten regions of interest (ROI) located near the plasma membrane

Next, we tested the hypothesis that Rho proteins might play a role in regulating the cellular distribution of pendrin. To this end, the membrane expression of pendrin was evaluated by FRET with a membrane probe (EYFP-Mem, see the "Methods" section). NCI-H292 cells were left untreated of stimulated with IL13 (50 ng/ml). Alternatively, cells were treated with IL13 in the presence of Y27632 (100 μM for 30 min), a selective inhibitor of Rho kinase, a downstream effector of Rho proteins. A significant decrease of NFRET signal was detected in cells co-treated with Y27632 and IL13 compared with cells incubated with IL13 alone (IL13-Y27632, 91.81 ± 2.392, n = 65 cells, vs. IL13, 109.9 ± 2.319, n = 211 cells, #p < 0.0001 Fig. 8a), therefore indicating that Y27632 abolished the effect of IL13 on pendrin abundance at the plasma membrane. These findings are also indicated as frequency distribution histogram of the relative changes of NFRET under the described conditions (Fig. 8b).

To better understand the molecular mechanism bridging pendrin, Rho signaling, and actin dynamics, we next investigated the co-immunolocalization of pendrin and actin by confocal microscopy (Fig. 9). These studies indicated that, compared with untreated cells, IL13 exposure stabilized actin cytoskeleton (red), which colocalized with pendrin (green). No relevant co-localization between pendrin and actin was observed following treatment with IL13 in the presence of

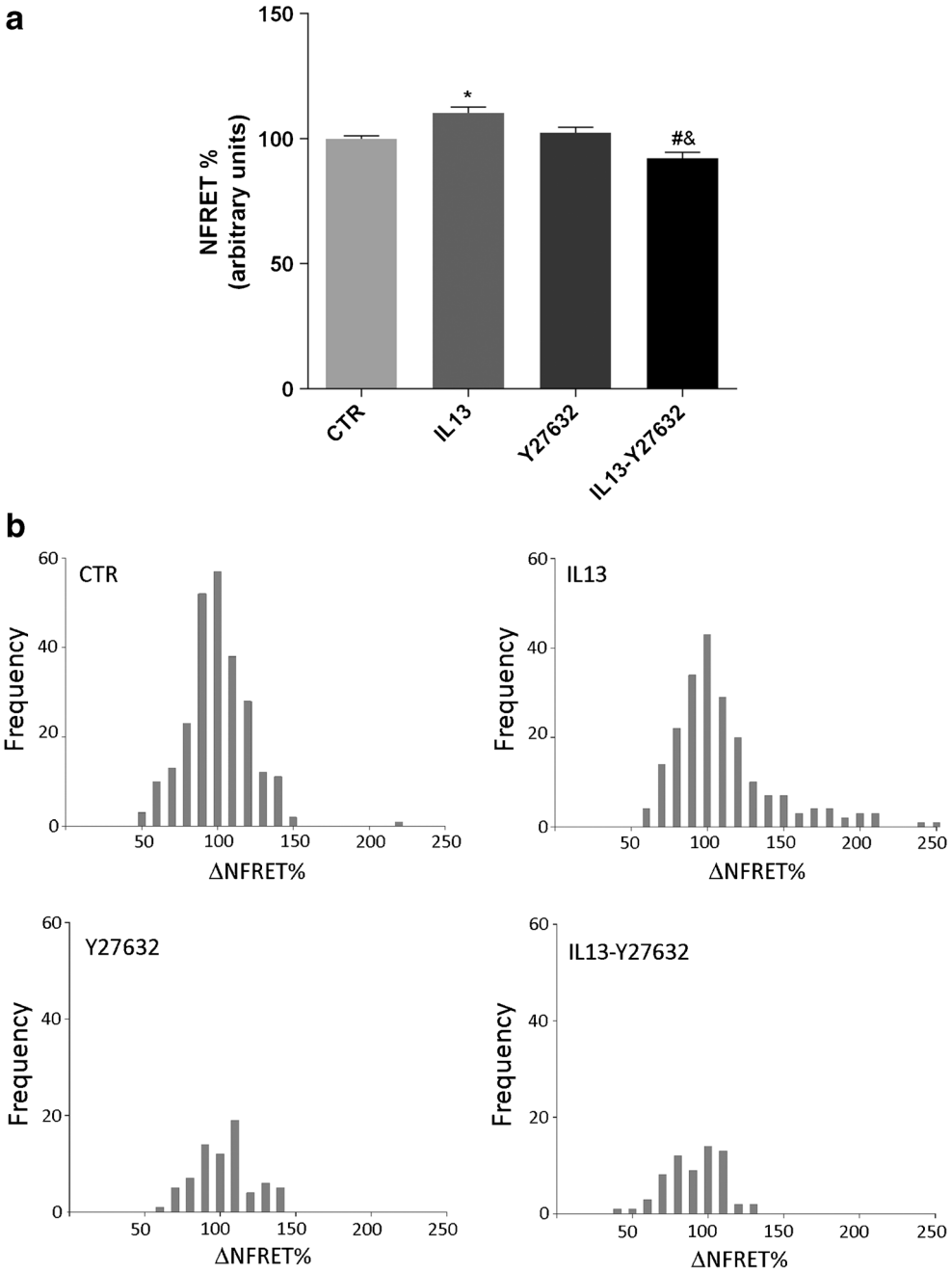

Fig. 8 Evaluation of pendrin expression at the plasma membrane by FRET studies in the presence or absence of IL3 and Y27632. **a** NCI-H292 cells were transiently transfected with PDS-ECFP and EYFP-Mem. FRET experiments were performed 48 h after transfection. Histograms represent NFRET determined in cells exposed to the vehicle (CTR), IL13 (50 ng/ml for 24 h), Y27632 (100 μM for 30 min), or IL13 and Y27632 (*$p < 0.001$ vs. CTR; $^{\#}p < 0.0001$ vs. IL13; $^{\&}p < 0.05$ vs. Y27632). **b** Frequency distribution histograms of the relative changes of NFRET in percent, under basal condition (CTR), IL13 stimulation, Y27632, and co-treatment with IL13 and Y27632. The obtained data were collected from ten regions of interest (ROI) located near the plasma membrane

theophylline, therefore indicating that theophylline prevented IL13 effect (Fig. 9).

To quantify the interaction between actin and pendrin, we performed FRET studies using pendrin N-terminally tagged with ECFP and actin C-terminally tagged with EYFP. In line with co-immunolocalization findings, IL13 increased the NFRET signal, which is consistent with an increased interaction between pendrin and actin. Exposure to theophylline decreased the binding of pendrin to actin induced by IL13 (Fig. 10).

Discussion

In this study, we provide evidence that IL13 stimulates the trafficking of the epithelial anion exchanger pendrin to the plasma membrane in NCI-H292 cells and that this effect is reversed by theophylline treatment. *Slc26a4*/pendrin expression was shown to be enhanced by IL4/IL13 and IL17A dependently or independently of STAT6 signaling in HEK-Blue cells and in the lungs of *B. pertussis*-infected mice, respectively [40, 49]. Here, in NCI-H292 cells, treatment with IL13 for

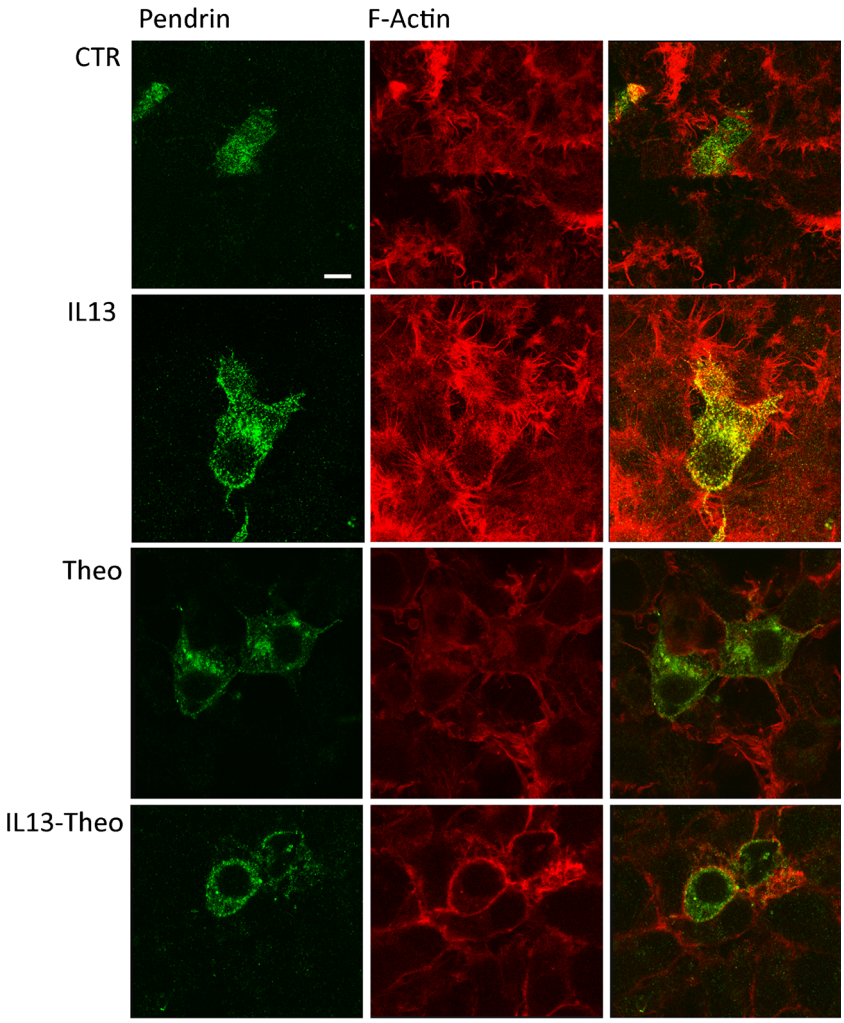

Fig. 9 Confocal analysis of F-actin and pendrin localization in NCI-H292 cells. Cells were transfected with PDS-ECFP and treated with the vehicle (CTR), IL13 (50 ng/ml for 24 h), theophylline (Theo, 10 μg/ml for 8 h), or IL13 and theophylline (IL13-Theo; 50 ng/ml IL13 for 24 h in the presence of 10 μg/ml theophylline for the last 8 h). Specimens were subjected to immunocytochemistry to detect pendrin and then incubated with Phalloidin-TRITC (400 μg/ml) for 45 min at room temperature to detect F-actin. Pendrin is visualized in *green* and actin in *red*. *Scale bar* 5 μM

24 h did not promote the expression of pendrin (no specific band corresponding to pendrin has been detected by immunoblotting analysis either in the presence or absence of IL13 stimulation, data not shown).

In the past few years, increasing evidence for the involvement of pendrin in respiratory disorders have been reported [27, 39, 49]. Pendrin knockout mice displayed a lower allergen-induced airway hyperreactivity and inflammation compared to control mice [38], despite the higher expression of inflammatory cytokines. During allergic response, IL13 alters chloride conductance [13], promotes mucus production, and electrolyte and water secretion into the airway surface liquid (ASL). Reduction of the ASL thickness, due to dehydration and/or abnormal ion transport, is associated with airway inflammation and obstruction. A recent report demonstrated that pendrin is involved in controlling ASL thickness, since pendrin deficiency significantly increased ASL thickness in IL13-stimulated mouse tracheal epithelial cells [38]. In line, selective pendrin inhibitors increased ASL in cystic fibrosis [23].

As previously mentioned, pendrin can exchange chloride for other anions such as iodide, hydroxide, thiocyanate, and bicarbonate [41, 53]. Bicarbonate has many important functions in the human body. In the respiratory system, bicarbonate secretion is needed for mucus secretion, mucin expansion, and mucosal protection [18, 22]. Altered pH/bicarbonate secretion may play a role in determining cystic fibrosis lung phenotype since low pH, due to aberrant bicarbonate secretion, decreases ciliary beat frequency [10], thus preventing bacterial removal by phagocytic cells [1]. Surprisingly, here we found that exposure to IL13 increased intracellular pH (Fig. 4), despite the increase of the cell surface expression of pendrin (Figs. 1, 2, and 3). We could think of two explanations for this finding. The first hypothesis is that exposure to IL13, similarly to IL4, changed the transport features of pendrin, thus promoting thiocyanate (SCN^-) instead of bicarbonate transport [41]. However, as assessed by anionic chromatography, SCN^- ions were not detected in the apical fluid of untreated and IL13-treated cells (data not shown).

Alternatively, IL13, similarly to other cytokines such as IL7 and IL3, may promote cellular alkalinization by stimulating NHE1 activity [28], consequently increasing reactive oxygen species (ROS) production via NADPH oxidase [33, 34].

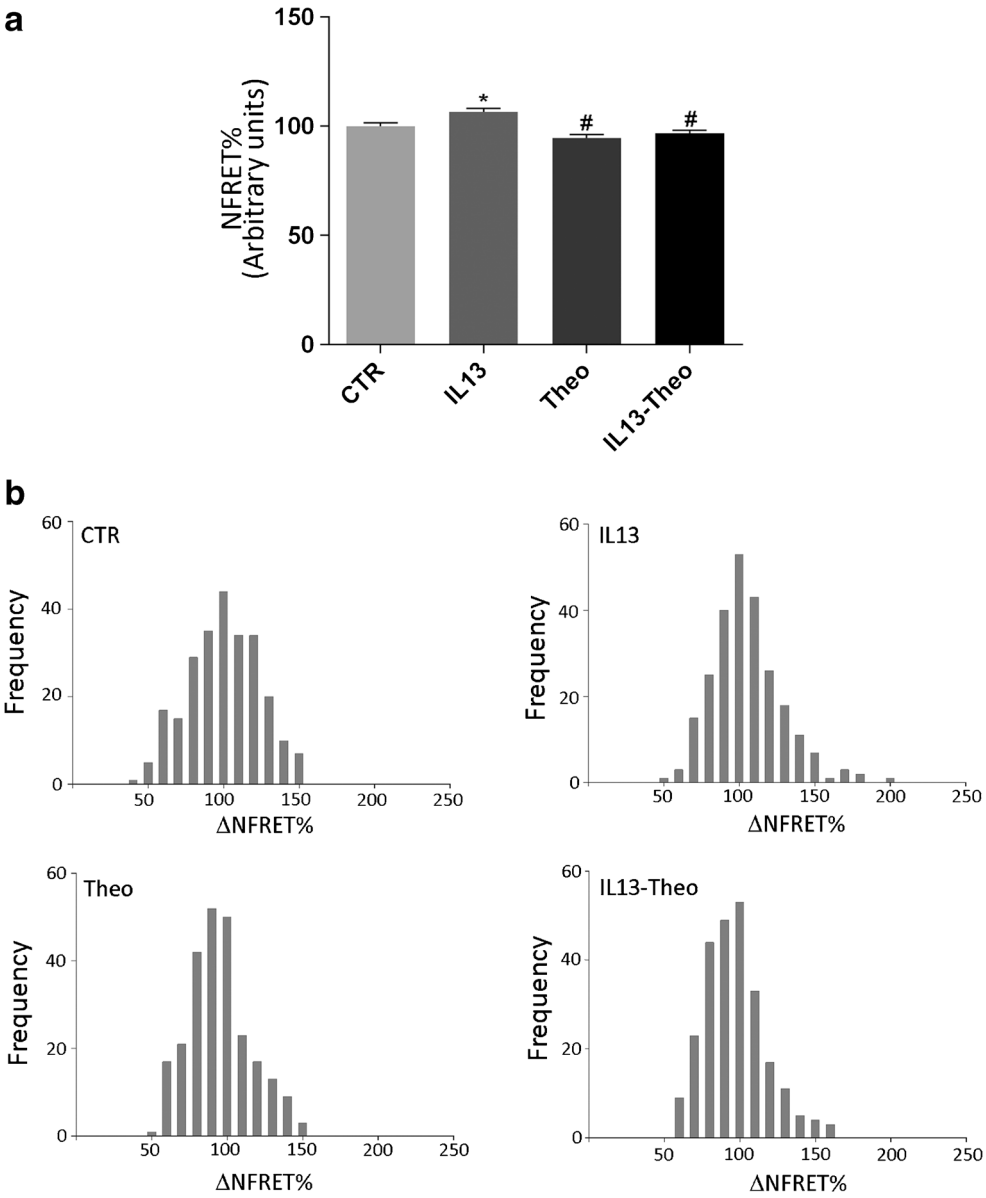

Fig. 10 Analysis of pendrin interaction with actin by FRET experiments. **a** NCI-H292 cells were co-transfected with ECFP-PDS and Actin-EYFP for 48 h and treated with the vehicle (CTR), IL13 (50 ng/ml for 24 h), theophylline (Theo, 10 μg/ml for 8 h), or IL13 and theophylline (IL13-Theo; 50 ng/ml IL13 for 24 h in the presence of 10 μg/ml theophylline for the last 8 h). (*$p < 0.05$ vs. CTR; #$p < 0.0001$ vs. IL13). **b** Frequency distribution histograms of the relative changes of NFRET in percent, under basal condition (CTR), IL13 stimulation, theophylline (Theo), and co-treatment with IL13 and theophylline (IL13-Theo). The obtained data were collected from ten regions of interest (ROI) located near the plasma membrane

In line, an increase of oxidant activity under IL13 exposure has been described in airway epithelial cells [14, 25] and in NCI-H292 cells (data not shown). Here, treatment with DMA, which inhibits NHE activity, revealed that cells expressing pendrin and treated with IL13 displayed a high extent of intracellular acidification, due to sustained bicarbonate extrusion. Importantly, IL13 increased intracellular pH only in cells expressing pendrin. These results let to conclude that IL13-dependent over-activation of pendrin may be associated with activation of NHE.

Upregulation of pendrin accompanied by elevated expression levels of inflammatory cytokines can be actually considered a signature of lung inflammation [16]. In lung diseases, the increased oxidative stress caused lack of response to glucocorticoids and decrease of the histone deacetylase (HDAC) activity [12]. Independently of phosphodiesterases inhibition, theophylline, at lower concentration, restored corticosteroids sensitivity and displayed an anti-inflammatory effect in asthma and COPD, by modulating the activation of the inflammatory mediator NF-kB and increasing the activity of HDAC [6]. In the present study, theophylline did not alter the basal intracellular cAMP level (data not shown), likely suggesting that the counteracting effect of theophylline on IL13 action may be due to its anti-inflammatory and antioxidant features.

Notably, in bronchial smooth muscle cells, IL13/STAT6 signaling increases cell contractility by augmenting the Rho pathway [9], which is actually considered an important therapeutic target for asthma [50]. Selective inhibitors of Rho kinase decreases IL13-induced airway inflammation and mucus secretion by modulating STAT6 [20, 50, 63]. In NCI-H292 cells, IL13 stimulates Rho proteins (Fig. 7), possibly via G-alpha-13 that activates NHE1 through a Rho-dependent

pathway [26]. Interestingly, treatment with Y27632, an inhibitor of Rho kinase, reduces IL13-induced pendrin abundance at the plasma membrane (Fig. 8), indicating the involvement of Rho signaling in modulating the cellular distribution of pendrin. At high concentration (100 μM), Y27632 not only inhibits Rho kinases but promotes the loss of actin stress fibers in human airway epithelial cells [43].

Rho-GTPases are known regulators of actin cytoskeleton [24, 44]. When active, Rho proteins can bind cell membranes and promote actin polymerization at discrete sites on the plasma membrane, thereby controlling membrane remodeling and trafficking of cellular proteins [45, 56]. To date, no actin-binding sites have been described in pendrin, even though its C-terminal domain holds a putative actin-binding sequence (DxI/LKKxT) similar to that observed in other actin-binding proteins such as cofilin [8, 64]. Our data demonstrate that IL13 stabilizes pendrin at the plasma membrane through the interaction with actin filaments, which are partially depolymerized with theophylline. A possible explanation is that the formation of cortical actin filaments, under L13 treatment, may slow the constitutive endocytosis of pendrin whereby stabilizing its plasma membrane localization (Figs. 1, 2, and 3). Indeed, actin depolymerization, obtained with theophylline or with Y27632 under IL13 treatment, is associated with a significant reduction of the abundance of pendrin at the plasma membrane.

In this respect, we have previously showed that inhibition of Rho, obtained after forskolin stimulation, resulted in intracellular acidification due to a significant increase of pendrin trafficking at the plasma membrane. These apparent discrepancies can be explained considering the dual and bidirectional role of actin cytoskeleton in controlling the constitutive exocytosis and endocytosis. Specifically, a partial depolymerization of the "cortical actin cage" may facilitate the constitutive exocytosis [37, 46, 56]. Conversely, IL13, by stimulating the formation of actin filaments (Fig. 9), might reduce the rate and the extent of the constitutive endocytosis. Therefore, the plasma membrane abundance of pendrin may be considered the result of a precise balance between the constitutive exocytosis and endocytosis. Nevertheless, an increase in the pendrin abundance at the cell membrane due to increased exocytosis or to decreased endocytosis did not modify the pendrin transport property as bicarbonate exchanger.

To conclude, the present studies highlight the pivotal role of IL13 in controlling airway remodeling, which is regulated by the integrated cooperation of different cells types that are target of IL13 action and includes the Rho signal pathway activation. Moreover, our observations propose a role of pendrin in modulating the intracellular pH and promoting respiratory inflammation.

Acknowledgements This study was funded by a grant from University of Bari, Italy (Idea Giovani 2011), by PRIN (Research Program of National Interest) projects to GT (Tamma01373409Prin) and by ASI (Italian Space Agency) grant (N. 2013-091-R.0) to GV.

Compliance with ethical standards

Conflict of interest The authors declare that they have no conflict of interest.

References

1. Alexis NE, Muhlebach MS, Peden DB, Noah TL (2006) Attenuation of host defense function of lung phagocytes in young cystic fibrosis patients. Journal of cystic fibrosis : official journal of the European Cystic Fibrosis Society 5:17–25
2. Anagnostopoulou P, Dai L, Schatterny J, Hirtz S, Duerr J, Mall MA (2010) Allergic airway inflammation induces a pro-secretory epithelial ion transport phenotype in mice. Eur Respir J 36:1436–1447
3. Astrand AB, Hemmerling M, Root J, Wingren C, Pesic J, Johansson E, Garland AL, Ghosh A, Tarran R (2015) Linking increased airway hydration, ciliary beating, and mucociliary clearance through ENaC inhibition. American journal of physiology Lung cellular and molecular physiology 308:L22–L32
4. Azroyan A, Laghmani K, Crambert G, Mordasini D, Doucet A, Edwards A (2011) Regulation of pendrin by pH: dependence on glycosylation. The Biochemical journal 434:61–72
5. Barnes PJ (2012) Severe asthma: advances in current management and future therapy. J Allergy Clin Immunol 129:48–59
6. Barnes PJ (2003) Theophylline: new perspectives for an old drug. Am J Respir Crit Care Med 167:813–818
7. Bazzini C, Benedetti L, Civello D, Zanoni C, Rossetti V, Marchesi D, Garavaglia ML, Paulmichl M, Francolini M, Meyer G, Rodighiero S (2014) ICln: a new regulator of non-erythroid 4.1R localisation and function. PLoS One 9:e108826
8. Bresnick AR, Warren V, Condeelis J (1990) Identification of a short sequence essential for actin binding by Dictyostelium ABP-120. J Biol Chem 265:9236–9240
9. Chiba Y, Nakazawa S, Todoroki M, Shinozaki K, Sakai H, Misawa M (2009) Interleukin-13 augments bronchial smooth muscle contractility with an up-regulation of RhoA protein. Am J Respir Cell Mol Biol 40:159–167
10. Clary-Meinesz C, Mouroux J, Cosson J, Huitorel P, Blaive B (1998) Influence of external pH on ciliary beat frequency in human bronchi and bronchioles. Eur Respir J 11:330–333
11. Corren J, Lemanske RF, Hanania NA, Korenblat PE, Parsey MV, Arron JR, Harris JM, Scheerens H, Wu LC, Su Z, Mosesova S, Eisner MD, Bohen SP, Matthews JG (2011) Lebrikizumab treatment in adults with asthma. N Engl J Med 365:1088–1098
12. Cosio BG, Tsaprouni L, Ito K, Jazrawi E, Adcock IM, Barnes PJ (2004) Theophylline restores histone deacetylase activity and steroid responses in COPD macrophages. J Exp Med 200:689–695
13. Danahay H, Atherton H, Jones G, Bridges RJ, Poll CT (2002) Interleukin-13 induces a hypersecretory ion transport phenotype in human bronchial epithelial cells. American journal of physiology Lung cellular and molecular physiology 282:L226–L236
14. Dickinson JD, Alevy Y, Malvin NP, Patel KK, Gunsten SP, Holtzman MJ, Stappenbeck TS, and Brody SL (2015) IL13 activates autophagy to regulate secretion in airway epithelial cells. Autophagy 0
15. Dossena S, Nofziger C, Lang F, Valenti G, Paulmichl M (2011) The ESF meeting on "The proteomics, epigenetics and pharmacogenetics of pendrin". Cellular physiology and biochemistry : international journal of experimental cellular physiology, biochemistry, and pharmacology 28:377–384
16. Ehrnthaller C, Flierl M, Perl M, Denk S, Unnewehr H, Ward PA, Radermacher P, Ignatius A, Gebhard F, Chinnaiyan A, Huber-Lang

M (2015) The molecular fingerprint of lung inflammation after blunt chest trauma. Eur J Med Res 20:70
17. Fugazzola L, Cerutti N, Mannavola D, Vannucchi G, Beck-Peccoz P (2001) The role of pendrin in iodide regulation. Exp Clin Endocrinol Diabetes 109:18–22
18. Garcia MA, Yang N, Quinton PM (2009) Normal mouse intestinal mucus release requires cystic fibrosis transmembrane regulator-dependent bicarbonate secretion. J Clin Invest 119:2613–2622
19. Garnett JP, Hickman E, Burrows R, Hegyi P, Tiszlavicz L, Cuthbert AW, Fong P, Gray MA (2011) Novel role for pendrin in orchestrating bicarbonate secretion in cystic fibrosis transmembrane conductance regulator (CFTR)-expressing airway serous cells. J Biol Chem 286:41069–41082
20. Gerthoffer WT, Solway J, Camoretti-Mercado B (2013) Emerging targets for novel therapy of asthma. Curr Opin Pharmacol 13:324–330
21. Gorrieri G, Scudieri P, Caci E, Schiavon M, Tomati V, Sirci F, Napolitano F, Carrella D, Gianotti A, Musante I, Favia M, Casavola V, Guerra L, Rea F, Ravazzolo R, Di Bernardo D, Galietta LJ (2016) Goblet cell hyperplasia requires high bicarbonate transport to support mucin release. Scientific reports 6:36016
22. Gustafsson JK, Ermund A, Ambort D, Johansson ME, Nilsson HE, Thorell K, Hebert H, Sjovall H, Hansson GC (2012) Bicarbonate and functional CFTR channel are required for proper mucin secretion and link cystic fibrosis with its mucus phenotype. J Exp Med 209:1263–1272
23. Haggie PM, Phuan PW, Tan JA, Zlock L, Finkbeiner WE, Verkman AS (2016) Inhibitors of pendrin anion exchange identified in a small molecule screen increase airway surface liquid volume in cystic fibrosis. FASEB journal : official publication of the Federation of American Societies for Experimental Biology 30: 2187–2197
24. Hall A (2012) Rho family GTPases. Biochem Soc Trans 40: 1378–1382
25. Harper RW, Xu C, Eiserich JP, Chen Y, Kao CY, Thai P, Setiadi H, Wu R (2005) Differential regulation of dual NADPH oxidases/peroxidases, Duox1 and Duox2, by Th1 and Th2 cytokines in respiratory tract epithelium. FEBS Lett 579:4911–4917
26. Hooley R, Yu CY, Symons M, Barber DL (1996) G alpha 13 stimulates Na+−H+ exchange through distinct Cdc42-dependent and RhoA-dependent pathways. J Biol Chem 271:6152–6158
27. Ishida A, Ohta N, Suzuki Y, Kakehata S, Okubo K, Ikeda H, Shiraishi H, Izuhara K (2012) Expression of pendrin and periostin in allergic rhinitis and chronic rhinosinusitis. Allergology international : official journal of the Japanese Society of Allergology 61:589–595
28. Khaled AR, Moor AN, Li A, Kim K, Ferris DK, Muegge K, Fisher RJ, Fliegel L, Durum SK (2001) Trophic factor withdrawal: p38 mitogen-activated protein kinase activates NHE1, which induces intracellular alkalinization. Mol Cell Biol 21:7545–7557
29. Kikuchi T, Shively JD, Foley JS, Drazen JM, Tschumperlin DJ (2004) Differentiation-dependent responsiveness of bronchial epithelial cells to IL-4/13 stimulation. American journal of physiology Lung cellular and molecular physiology 287:L119–L126
30. Krane CM, Deng B, Mutyam V, McDonald CA, Pazdziorko S, Mason L, Goldman S, Kasaian M, Chaudhary D, Williams C, Ho MW (2009) Altered regulation of aquaporin gene expression in allergen and IL-13-induced mouse models of asthma. Cytokine 46:111–118
31. Kuperman DA, Lewis CC, Woodruff PG, Rodriguez MW, Yang YH, Dolganov GM, Fahy JV, Erle DJ (2005) Dissecting asthma using focused transgenic modeling and functional genomics. J Allergy Clin Immunol 116:305–311
32. Lacroix L, Mian C, Caillou B, Talbot M, Filetti S, Schlumberger M, Bidart JM (2001) Na(+)/I(−) symporter and Pendred syndrome gene and protein expressions in human extra-thyroidal tissues. European journal of endocrinology / European Federation of Endocrine Societies 144:297–302
33. Liu R, Carretero OA, Ren Y, Wang H, Garvin JL (2008) Intracellular pH regulates superoxide production by the macula densa. Am J Physiol Renal Physiol 295:F851–F856
34. Liu R, Garvin JL, Ren Y, Pagano PJ, Carretero OA (2007) Depolarization of the macula densa induces superoxide production via NAD(P)H oxidase. Am J Physiol Renal Physiol 292:F1867–F1872
35. Lozano R, Ortblad KF, Lopez AD, Murray CJ (2013) Mortality from HIV in the Global Burden of Disease study—authors' reply. Lancet 381:991–992
36. Meyers DA, Bleecker ER, Holloway JW, Holgate ST (2014) Asthma genetics and personalised medicine. Lancet Respir Med 2:405–415
37. Moore M, Marroquin BA, Gugliotta W, Tse R, White SR (2004) Rho kinase inhibition initiates apoptosis in human airway epithelial cells. Am J Respir Cell Mol Biol 30:379–387
38. Nakagami Y, Favoreto S Jr, Zhen G, Park SW, Nguyenvu LT, Kuperman DA, Dolganov GM, Huang X, Boushey HA, Avila PC, Erle DJ (2008) The epithelial anion transporter pendrin is induced by allergy and rhinovirus infection, regulates airway surface liquid, and increases airway reactivity and inflammation in an asthma model. J Immunol 181:2203–2210
39. Nakao I, Kanaji S, Ohta S, Matsushita H, Arima K, Yuyama N, Yamaya M, Nakayama K, Kubo H, Watanabe M, Sagara H, Sugiyama K, Tanaka H, Toda S, Hayashi H, Inoue H, Hoshino T, Shiraki A, Inoue M, Suzuki K, Aizawa H, Okinami S, Nagai H, Hasegawa M, Fukuda T, Green ED, Izuhara K (2008) Identification of pendrin as a common mediator for mucus production in bronchial asthma and chronic obstructive pulmonary disease. J Immunol 180:6262–6269
40. Nofziger C, Vezzoli V, Dossena S, Schonherr T, Studnicka J, Nofziger J, Vanoni S, Stephan S, Silva ME, Meyer G, Paulmichl M (2011) STAT6 links IL-4/IL-13 stimulation with pendrin expression in asthma and chronic obstructive pulmonary disease. Clin Pharmacol Ther 90:399–405
41. Pedemonte N, Caci E, Sondo E, Caputo A, Rhoden K, Pfeffer U, Di Candia M, Bandettini R, Ravazzolo R, Zegarra-Moran O, Galietta LJ (2007) Thiocyanate transport in resting and IL-4-stimulated human bronchial epithelial cells: role of pendrin and anion channels. J Immunol 178:5144–5153
42. Pezzulo AA, Tang XX, Hoegger MJ, Alaiwa MH, Ramachandran S, Moninger TO, Karp PH, Wohlford-Lenane CL, Haagsman HP, van Eijk M, Banfi B, Horswill AR, Stoltz DA, McCray PB Jr, Welsh MJ, Zabner J (2012) Reduced airway surface pH impairs bacterial killing in the porcine cystic fibrosis lung. Nature 487:109–113
43. Procino G, Milano S, Tamma G, Dossena S, Barbieri C, Nicoletti MC, Ranieri M, Di Mise A, Nofziger C, Svelto M, Paulmichl M, Valenti G (2013) Co-regulated pendrin and aquaporin 5 expression and trafficking in Type-B intercalated cells under potassium depletion. Cellular physiology and biochemistry : international journal of experimental cellular physiology, biochemistry, and pharmacology 32:184–199
44. Ridley AJ (2006) Rho GTPases and actin dynamics in membrane protrusions and vesicle trafficking. Trends Cell Biol 16:522–529
45. Ridley AJ (2001) Rho proteins: linking signaling with membrane trafficking. Traffic 2:303–310
46. Ritter M, Ravasio A, Jakab M, Chwatal S, Furst J, Laich A, Gschwentner M, Signorelli S, Burtscher C, Eichmuller S, Paulmichl M (2003) Cell swelling stimulates cytosol to membrane transposition of ICln. J Biol Chem 278:50163–50174
47. Rodighiero S, Bazzini C, Ritter M, Furst J, Botta G, Meyer G, Paulmichl M (2008) Fixation, mounting and sealing with nail polish of cell specimens lead to incorrect FRET measurements using acceptor photobleaching. Cellular physiology and biochemistry : international journal of experimental cellular physiology, biochemistry, and pharmacology 21:489–498

48. Rodighiero S, Botta G, Bazzini C, Meyer G (2011) Pendrin overexpression affects cell volume recovery, intracellular pH and chloride concentration after hypotonicity-induced cell swelling. Cellular physiology and biochemistry : international journal of experimental cellular physiology, biochemistry, and pharmacology 28:559–570
49. Scanlon KM, Gau Y, Zhu J, Skerry C, Wall SM, Soleimani M, Carbonetti NH (2014) Epithelial anion transporter pendrin contributes to inflammatory lung pathology in mouse models of Bordetella pertussis infection. Infect Immun 82:4212–4221
50. Schaafsma D, Gosens R, Zaagsma J, Halayko AJ, Meurs H (2008) Rho kinase inhibitors: a novel therapeutical intervention in asthma? Eur J Pharmacol 585:398–406
51. Scott DA, Wang R, Kreman TM, Sheffield VC, Karniski LP (1999) The Pendred syndrome gene encodes a chloride-iodide transport protein. Nat Genet 21:440–443
52. Shaw JG, Vaughan A, Dent AG, O'Hare PE, Goh F, Bowman RV, Fong KM, Yang IA (2014) Biomarkers of progression of chronic obstructive pulmonary disease (COPD). Journal of thoracic disease 6:1532–1547
53. Soleimani M, Greeley T, Petrovic S, Wang Z, Amlal H, Kopp P, Burnham CE (2001) Pendrin: an apical Cl−/OH−/HCO3-exchanger in the kidney cortex. Am J Physiol Renal Physiol 280:F356–F364
54. Stanley A, Thompson K, Hynes A, Brakebusch C, Quondamatteo F (2014) NADPH oxidase complex-derived reactive oxygen species, the actin cytoskeleton, and Rho GTPases in cell migration. Antioxid Redox Signal 20:2026–2042
55. Tamma G, Carmosino M, Svelto M, Valenti G (2005) Bradykinin signaling counteracts cAMP-elicited aquaporin 2 translocation in renal cells. Journal of the American Society of Nephrology : JASN 16:2881–2889
56. Tamma G, Klussmann E, Maric K, Aktories K, Svelto M, Rosenthal W, Valenti G (2001) Rho inhibits cAMP-induced translocation of aquaporin-2 into the apical membrane of renal cells. Am J Physiol Renal Physiol 281:F1092–F1101
57. Tamma G, Lasorsa D, Ranieri M, Mastrofrancesco L, Valenti G, Svelto M (2011) Integrin signaling modulates AQP2 trafficking via Arg-Gly-Asp (RGD) motif. Cellular physiology and biochemistry : international journal of experimental cellular physiology, biochemistry, and pharmacology 27:739–748
58. Tamma G, Lasorsa D, Trimpert C, Ranieri M, Di Mise A, Mola MG, Mastrofrancesco L, Devuyst O, Svelto M, Deen PM, Valenti G (2014) A protein kinase A-independent pathway controlling aquaporin 2 trafficking as a possible cause for the syndrome of inappropriate antidiuresis associated with polycystic kidney disease 1 haploinsufficiency. Journal of the American Society of Nephrology : JASN 25:2241–2253
59. Tamma G, Ranieri M, Dossena S, Di Mise A, Nofziger C, Svelto M, Paulmichl M, Valenti G (2013) A FRET-based approach for quantitative evaluation of forskolin-induced pendrin trafficking at the plasma membrane in bronchial NCI H292 cells. Cellular physiology and biochemistry : international journal of experimental cellular physiology, biochemistry, and pharmacology 32:200–209
60. Vaiskunaite R, Adarichev V, Furthmayr H, Kozasa T, Gudkov A, Voyno-Yasenetskaya TA (2000) Conformational activation of radixin by G13 protein alpha subunit. J Biol Chem 275:26206–26212
61. Voyno-Yasenetskaya T, Conklin BR, Gilbert RL, Hooley R, Bourne HR, Barber DL (1994) G alpha 13 stimulates Na-H exchange. J Biol Chem 269:4721–4724
62. Wang CC, Ng CP, Shi H, Liew HC, Guo K, Zeng Q, Hong W (2010) A role for VAMP8/endobrevin in surface deployment of the water channel aquaporin 2. Mol Cell Biol 30:333–343
63. Xie T, Luo G, Zhang Y, Wang X, Wang X, Wu M, Li G (2015) Rho-kinase inhibitor fasudil reduces allergic airway inflammation and mucus hypersecretion by regulating STAT6 and NFkappaB. Clinical and experimental allergy : journal of the British Society for Allergy and Clinical Immunology 45:1812–1822
64. Yonezawa N, Nishida E, Ohba M, Seki M, Kumagai H, Sakai H (1989) An actin-interacting heptapeptide in the cofilin sequence. European journal of biochemistry / FEBS 183:235–238
65. Yoshizaki H, Ohba Y, Kurokawa K, Itoh RE, Nakamura T, Mochizuki N, Nagashima K, Matsuda M (2003) Activity of Rho-family GTPases during cell division as visualized with FRET-based probes. J Cell Biol 162:223–232